Published in final edited form as:
J Biol Chem. 2005 December 9; 280(49): 40788–40795. doi:10.1074/jbc.M504765200.

An Aberrant Sequence in a Connexin46 Mutant Underlies Congenital Cataracts*

Peter J. Minogue‡, **Xiaoqin Liu**§, **Lisa Ebihara**§, **Eric C. Beyer**‡, and **Viviana M. Berthoud**[1,‡]

‡ Department of Pediatrics, University of Chicago, Chicago, Illinois 60637

§ Department of Physiology and Biophysics, Rosalind Franklin University of Medicine and Science, North Chicago, Illinois 60064

Abstract

An increasing number of diseases have been mapped to genes coding for ion channel proteins, including the gap junction proteins, connexins. Here, we report on the identification of an amino acid sequence underlying the behavior of a non-functional mutant connexin46 (CX46) associated with congenital cataracts. The mutant protein, CX46fs380, is 31 amino acids longer than CX46 and contains 87 aberrant amino acids in its C terminus. When expressed in mammalian cells, the mutant CX46 was not found at gap junctional plaques, but it showed extensive co-localization with markers for ERGIC and Golgi. The severe reductions in function and formation of gap junctional plaques were transferred to other connexins by creating chimeras containing the last third (or more) of the aberrant C terminus of the CX46 mutant. This sequence also impaired trafficking of a CD8 chimera. Site-directed mutagenesis of a diphenylalanine restored appositional membrane localization and function. These results suggest a novel mechanism in which a mutation causes disease by generating a motif that leads to retention within the synthetic/secretory pathway.

Gap junctions are membrane specializations that contain intercellular channels that allow transfer of ions and small molecules between cells. Hemichannels contributed by two closely apposed cells dock to form gap junction channels. Each hemichannel is a hexamer of subunit proteins named connexins (CX).[2] Similar to other integral membrane proteins, connexins are synthesized in the rough endoplasmic reticulum and follow the secretory pathway to the plasma membrane. Connexins oligomerize into hexamers during their transit through the endoplasmic reticulum/Golgi compartments and they are inserted into the plasma membrane as hemichannels. Once there, a hemichannel from one cell can dock with another from a closely apposed cell to form a gap junction channel. Channels can cluster at appositional membranes and form gap junctional plaques (1).

Mutations in several ion channel proteins have been associated with human diseases (2). Congenital cataracts have been mapped to several genes including those of connexins (3). One such mutation induces a frameshift in CX46 (4), a lens gap junction protein. The mutant protein, CX46fs380, is 31 amino acids longer than wild-type CX46 and contains a sequence of 87

*This work was supported by National Institutes of Health Grants EY08368 (to E. C. B.) and EY10589 (to L. E.).

1To whom correspondence should be addressed: Dept. of Pediatrics, Section of Hematology/Oncology, University of Chicago, 5841 S. Maryland Ave., MC 4060, Chicago, IL 60637. Tel.: 773-702-6808; Fax: 773-702-9881; E-mail: E-mail: vberthou@peds.bsd.uchicago.edu.

2The abbreviations used are: CX, connexin; BFA, Brefeldin A; CHX, cycloheximide; CT, C terminus; fs, frameshift; CX46CT, amino acids 380 – 435 of wild-type CX46; fs380CT, amino acid sequence of the C terminus of CX46fs380 after the frameshift; NGS, normal goat serum; PDI, protein-disulfide isomerase; PBS, phosphate-buffered saline, pH 7.4; g_j, junctional conductance; FITC, fluorescein isothiocyanate; ER, endoplasmic reticulum.

aberrant amino acids starting at residue 380. We have demonstrated that CX46fs380 is unable to induce hemi-gap junctional or junctional currents when expressed in *Xenopus* oocytes (5).

Several disease-associated mutant connexins have been reported in the past few years. These studies have shown that some traffic properly and reach the plasma membrane, but others are found in the endoplasmic reticulum or Golgi apparatus (6–14). The present experiments were designed to study the basis of the CX46fs380 malfunction.

EXPERIMENTAL PROCEDURES

Generation of Connexin Chimeras

Chimeras were generated by PCR using LA TAK DNA polymerase (Invitrogen) and cloned pfu DNA polymerase (Stratagene, La Jolla, CA) with the primers listed in TABLE ONE and the strategy outlined in TABLE TWO. All constructs were fully sequenced at the Cancer Research Center DNA Sequencing Facility of the University of Chicago to ensure that PCR amplification did not introduce random mutations.

Chemicals

All chemicals were obtained from Sigma unless otherwise specified.

Cell Culture

HeLa cells were grown as previously described (12). Connexin DNAs were subcloned into pcDNA3.1/Hygro(+) (Invitrogen). Transfections were carried out using Lipofectin following the manufacturer's directions (Invitrogen). Transiently transfected cells were grown for 40–48 h before processing for immunofluorescence. For stable transfection, clones were selected by their resistance to hygromycin (Calbiochem-Novabiochem Corporation, San Diego, CA).

Antibodies

Mouse monoclonal anti-protein-disulfide isomerase (PDI) antibody was obtained from Affinity Bioreagents (Golden, CO). Mouse monoclonal anti-Golgi 58K protein (clone 58K-9) was obtained from Sigma. Mouse monoclonal anti-ERGIC-53 antibody was obtained from Axxora LLC (San Diego, CA). The mouse monoclonal anti-LAMP-1 antibody developed by J. Thomas August and James E. K. Hildreth was obtained from the Developmental Studies Hybridoma Bank developed under the auspices of the NICHD and maintained by The University of Iowa, Department of Biological Sciences, Iowa City, IA 52242. Rabbit polyclonal anti-Cx32 antibodies were obtained from Invitrogen. Cy3-conjugated goat anti-mouse IgG and Cy2-conjugated goat anti-rabbit IgG antibodies were obtained from Jackson ImmunoResearch (West Grove, PA). FITC-conjugated mouse monoclonal anti-human CD8 antibody was obtained from BD Biosciences Pharmingen (San Diego, CA).

Generation of Anti-CX46, Anti-CX46fs380, and Anti-CX56CT Antibodies

To obtain anti-CX46 antibodies, a CX46 intracellular loop (CX46IL) peptide (including amino acids 120–136) coupled to KLH was used for rabbit immunization, and the serum obtained was affinity-purified through a Sulfolink column after coupling the CX46IL peptide following the manufacturer's directions (Pierce). To obtain anti-CX46fs380 and anti-CX56CT antibodies, glutathione *S*-transferase fusion proteins containing amino acids 379–466 of CX46fs380 or amino acids 255–511 of CX56 (15) were produced and used for rabbit immunization. These rabbit sera were stripped of anti-GST antibodies using a GST-immobilized agarose column (Pierce). For the anti-CX46fs380 antibodies, the stripped serum was affinity-purified using the CX46fs380 fusion protein coupled to a Sulfolink column (Pierce).

Immunofluorescence

Cells plated on 4-well chamber slides (LAB TEK, Nalge Nunc International, Naperville, IL) were allowed to reach 80–90% confluence.

Retention Signal in a Connexin Mutant

Hela cells were fixed in 4% paraformaldehyde. After fixation, cells were permeabilized with 1% Triton X-100 in phosphate-buffered saline pH 7.4 (PBS), blocked in 4% normal goat serum (NGS), 1% Triton X-100 in PBS, and incubated overnight in primary antibodies at 4 °C. Cells were then rinsed six times with PBS and incubated in Cy2- and/or Cy3-conjugated secondary antibodies. After incubation at room temperature for 45 min, cells were rinsed six times with PBS, and coverslips were mounted with 2% *n*-propylgallate in PBS/glycerol (1:1).

When using the FITC-conjugated mouse monoclonal anti-human CD8 antibody, HeLa cells stably transfected with CD8 chimeras were fixed in 100% methanol at −20 °C, blocked in 10% NGS in PBS, and incubated in antibody for 45 min. Then, cells were washed four times with PBS and coverslips mounted as above.

Specimens were studied with a Zeiss Plan Apochromat ×40 objective (n.a., 1.0) in an Axioplan 2 microscope (Carl Zeiss, München, Germany) equipped with a mercury lamp. Images were captured with an Axiocam digital camera (Carl Zeiss) using Zeiss AxioVision software. Confocal images were obtained using an IX70 Olympus Fluoview 200 laser-scanning confocal microscope (Melville, NY) equipped with laser lines (488 nm, 543 nm, 633 nm) with a ×60 Plan Apochromat objective (n.a., 1.4). Overlap images were generated using Image J software and the co-localization threshold plugin created by Tony Collins, Wayne Rasband, and Kevin Baler (University Health Network). Composite figures were assembled using Adobe Photoshop software (Adobe Systems, San Jose, CA).

Immunofluorescence was performed in transiently transfected cells at least three times for each construct, and at least in four different clones for stably transfected cells. Specimens were examined by three different observers, one of whom looked at all the visual fields in the well whereas the others looked at a minimum of 20 fields for each construct/treatment.

Cell Treatments

Brefeldin A—HeLa cells stably transfected with CX46fs380, Cx32-fs380CT, or CD8-fs380CT were treated with 40 μg/ml cycloheximide (CHX) for 16 h followed by incubation in the presence of 4 μg/ml BFA or ethanol (used as a solvent for the BFA stock solution) for 8 h or 20 h. These experiments were repeated three times for the CX46fs380 clones, and twice for the other chimeric constructs using at least two different concentrations of BFA (4 and 10 μg/ml).

Incubation at Reduced Temperatures—Cells were grown at 37 °C until they reached 40–50% confluence. Then, they were either transferred to 25 °C or 30 °C or left at 37 °C and further incubated until they reached 80–90% confluence as previously described (12). These experiments were performed three times.

Sodium 4-Phenylbutyrate—Cells were treated with 1, 4, or 16 mM sodium 4-phenylbutyrate (dissolved in water) for 24 h. These experiments were performed twice using each concentration.

After the treatments, cells were rinsed in PBS, fixed in 4% paraformaldehyde, and processed for immunofluorescence as described above.

Electrophysiological Measurements

The DNA constructs were subcloned into the RNA expression vector, SP64TII. The plasmids were linearized with SalI, and capped RNAs were synthesized using the mMessage mMachine SP6 *in vitro* transcription kit (Ambion, Austin, TX) according to the manufacturer's instructions. The amount of RNA was quantitated by measuring the absorbance at 260 nm.

Xenopus oocytes were prepared and tested as described previously (16). To measure the junctional conductance, cell pairs were studied using the dual two microelectrode technique (17). For simple measurements of gap junctional coupling, both cells of the pair were initially held at −40 mV and 5–10-mV steps were applied to one cell while holding the second cell at −40 mV. The junctional conductance (g_j) equals I_j/V_j, where $V_j = V_{cell2} - V_{cell1}$. Data acquisition and analysis were conducted using a personal computer running pCLAMP version 6.0.5 (Axon Instruments, Union City, CA). Microelectrodes were filled with 3 M KCl (pH 7.4) and had resistances of 0.2–2 MΩ. The bath solution was modified Barth's solution. All of the experiments were performed on oocytes previously injected with antisense Cx38 oligonucleotides to ensure that the observed currents were not caused by the expression of endogenous Cx38 (18). Data expressed as log(conductance) were analyzed for their statistical significance using the unpaired Student's *t* test.

Flow Cytometry Analysis

Batch clones of HeLa cells transfected with CD8 chimeras plated on 60-mm culture dishes were grown until 80% confluence. Cells were trypsinized, centrifuged, and the pellets incubated in 10% NGS in PBS for 10 min followed by incubation in FITC-conjugated mouse monoclonal anti-human CD8 antibody. After 20 min, cells were pelleted, rinsed twice with 10% NGS in PBS, and resuspended in 10% NGS in PBS. Prior to flow cytometry analysis, cells were stained with propidium iodide. Flow cytometry was carried out on a BD FACSCan flow cytometer (BD Biosciences, Rockville, MD). FITC fluorescence was acquired using the FL1 channel, and the data analyzed using FlowJo software. Similar results were obtained when repeating these experiments using different concentrations of antibody; the experiment was performed twice at the concentration shown.

RESULTS

The Mutant CX46 Is Impaired in Its Ability to Reach the Plasma Membrane

To test whether CX46fs380 formed non-functional channels or its trafficking to the plasma membrane was impaired, we examined the distribution of wild-type CX46 and CX46fs380 by immunofluorescence in transfected HeLa cells that are competent for formation of gap junctions. Whereas cells transfected with CX46 showed gap junctional plaques at appositional membranes, no gap junctional plaques were observed in cells transfected with CX46fs380 (Fig. 1*A*, *left* and *right panels*). Rather, CX46fs380 localized mostly in an intracellular location that corresponded to ERGIC and Golgi compartments based on its overlap with ERGIC-53 and the Golgi 58K protein (Fig. 1*B*). A minor proportion of CX46fs380 overlapped with the ER-resident protein PDI (not shown). The localization of CX46fs380 in the Golgi was further confirmed when it redistributed together with the Golgi 58K protein after treatment of transfected cells with BFA (Fig. 1*C*).

Several mutant membrane proteins have trafficking/folding defects that can be overcome by incubation at lower temperatures or treatment with chemical chaperones (19,20). To test whether the intracellular distribution of CX46fs380 was caused by its inability to acquire the correct conformation, we analyzed the cellular localization of CX46fs380 after incubation of the transfected cells at 25 or 30 °C or after treatment with sodium 4-phenylbutyrate. No

CX46fs380 immunoreactive gap junctional plaques were observed after any of these treatments (data not shown).

The Aberrant Behavior Results from Gain of a Deleterious Function

Because CX46fs380 lacks amino acids 380 – 435 of wild-type CX46, it was possible that the defects of CX46fs380 resulted from the absence of sequence signals contained in the missing wild-type region that allow efficient trafficking and formation of gap junctional plaques or to the presence of a sequence motif in the aberrant region that prevents proper trafficking/localization. To differentiate between these possibilities, we generated a truncated form of CX46 containing only the first 379 amino acids of wild-type CX46 (CX46tr380) and analyzed its distribution by immunofluorescence. Cells transfected with this construct showed gap junctional plaques (Fig. 1*A*, *center panel*). Therefore, we reasoned that the amino acid sequence of the CX46fs380 C terminus following the frameshift was responsible for the observed effects.

The Amino Acid Sequence after the Frameshift (fs380CT) Confers Abnormal Behavior to Connexin Chimeras

To test whether the aberrant localization and loss of function were transferable traits controlled by the abnormal C terminus of CX46fs380, we generated several constructs on the backbone of CX56 (the chicken orthologue of human CX46) and studied their cellular distribution. Immunofluorescent studies showed that anti-CX56 immunoreactivity localized at appositional membranes in HeLa cells transfected with wild-type CX56 (Fig. 2, *top left panel*). Cells transfected with CX56 truncated after amino acid 445 (CX56tr446), a position analogous to amino acid 380 in CX46, also showed anti-CX56 immunostaining at appositional membranes (Fig. 2, *top right panel*). Cells transfected with a chimera containing amino acids 380–435 of wild-type CX46 (CX46CT) appended to the first 445 amino acids of CX56 (CX56-CX46CT) also localized to appositional membranes (Fig. 2, *bottom left panel*). However, a chimera containing the aberrant sequence of the C terminus of CX46fs380 (CX56-fs380CT) showed an intracellular localization; its distribution was similar to that of CX46fs380 (compare Fig. 2, *bottom right panel* with Fig. 1*A*, *right panel*). The CX56 constructs were also analyzed for their ability to form functional gap junction channels in pairs of *Xenopus* oocytes. Wild-type CX56 induced large gap junctional conductances between oocyte pairs (Fig. 3*A*). CX56tr446 and the CX56-CX46CT chimera also induced large junctional conductances that were not significantly different from those induced by CX56 (Fig. 3, *A* and *B*). However, when CX56-fs380CT was expressed in *Xenopus* oocytes, gap junctional conductances were reduced to 7.6% of wild-type CX56 and 6.3% of CX56-CX46CT conductances (Fig. 3*B*), but they were still significantly higher than the junctional conductance determined in pairs of antisense Cx38-injected oocytes (Fig. 3*C*).

We also generated Cx32 chimeras in which CX46CT or fs380CT were appended to full-length Cx32 and characterized their behavior by immunofluorescence after transfection into HeLa cells. Whereas anti-Cx32 immunoreactivity localized to appositional membranes in cells transfected with Cx32-CX46CT (data not shown), it showed an intra-cellular localization in cells transfected with Cx32-fs380CT (Fig. 4*A*). The pattern of Cx32-fs380CT immunoreactivity resembled that of the ER showing a reticular staining throughout the cell. Extensive overlap of the immunoreactivities to anti-CX46fs380 and anti-PDI antibodies was observed (Fig. 4*A*). There was a rather poor correspondence between anti-Cx32 immunoreactivity and that of markers for ERGIC or Golgi compartment, but a minor amount of anti-Cx32 immunoreactivity overlapped with LAMP-1 in a small subpopulation of cells (not shown). When CHX-treated cells stably transfected with Cx32-fs380CT were allowed to recover in control media for 8 h, a weak diffuse signal throughout the cytoplasm with a brighter staining localized to the perinuclear region was observed. However, when BFA was present during the recovery phase, the Cx32-fs380CT immunoreactivity redistributed throughout the

cell (not shown) implying that Cx32-fs380CT initially reaches a BFA-sensitive Golgi compartment to be subsequently relocated to the ER where it predominantly resides at steady state. Functional characterization of these chimeras showed a drastic decrease in junctional conductance in oocyte pairs injected with Cx32-fs380CT cRNA as compared with that induced in oocyte pairs injected with Cx32-CX46CT cRNA (Fig. 4*B*). The junctional conductances induced by Cx32-fs380CT were not significantly different than those induced in antisense Cx38-injected oocytes.

The Last Third of fs380CT Confers Aberrant Behavior

To define sequence elements responsible for loss of appositional membrane localization and function, several CX56 chimeras containing different regions of the C terminus of CX46fs380 were generated and analyzed by immunofluorescence. Chimeras containing the first one-third (CX56-fs380(1–29)) or two-thirds (CX5-6fs380(1–58)) of fs380CT localized to appositional membranes like the chimera containing CX46CT (Fig. 5*A*). However, a CX56 chimera containing only the last 29 amino acids of the aberrant C terminus of CX46fs380 (CX56-fs380 (59–87)) localized within the cytoplasm (Fig. 5*A*).

These chimeras were also tested for their ability to induce junctional conductance in the *Xenopus* oocyte system. The chimera containing the first two-thirds of fs380CT (CX56-fs380 (1–58)) induced robust junctional conductances that were not significantly different from those induced by wild-type CX56 (Fig. 5*B*). However, the chimera containing the last third of fs380CT (CX56-fs380(59–87)) induced significantly reduced junctional conductances (Fig. 5*C*).

Identification of Amino Acid Residues Critical for the Abnormal Behavior

Examination of the last 29 amino acids of the C terminus of CX46fs380 revealed sequences that resembled previously described trafficking motifs (Fig. 6*A*). To test the possibility that these residues were responsible for the altered behavior of CX46fs380, the localization and function of chimeras in which these putative motifs were mutated was analyzed. Mutation of the amino acids TKTK (a dilysine-like motif) to TATA yielded a CX56 chimera (CX56-fs380TATA) that still localized intracellularly when transfected into HeLa cells (Fig. 6*B*). This chimera was not functional in oocyte pairs (Fig. 6*C*). However, distinct immunoreactive staining at appositional membranes was observed in HeLa cells expressing a CX56 chimera in which the FF in the C terminus of CX46fs380 was mutated to AA (CX56-fs380AA) (Fig. 6*B*). Moreover, CX56-fs380AA induced robust gap junctional currents; the macroscopic gap junctional conductance of oocyte pairs expressing the CX56-fs380AA chimera was not significantly different from the value obtained from wild-type CX56 (Fig. 6*C*).

To test whether the diphenylalanine was also responsible for the behavior of the other connexin constructs, these two amino acids were mutated toalaninesinCx32-fs380CTandCX46fs380. Similartotheresultsobtained with the CX56 chimera, Cx32-fs380AA (a Cx32 chimera in which the FF was replaced by AA) showed localization at appositional membranes (Fig. 7, *upper panels*) and functional gap junction channels (g_j: 24.37 ± 6.2 μS, n = 9). Moreover, replacement of FF in CX46fs380 with AA (CX46fs380AA) restored appositional membrane localization (Fig. 7, *bottom panels*) and function (g_j: 2.75 ± 0.37 μS, n = 8).

The Aberrant Sequence in CX46fs380 Causes Retention of a CD8 Chimera

A strategy used to study amino acid sequences that act as “retention” or “export” motifs has been to create chimeras with single transmembrane domain proteins such as CD8 (21). To test whether fs380CT affected trafficking of this unrelated protein, we generated a CD8 chimera containing fs380CT and stably transfected it into HeLa cells. Immunofluorescent studies in paraformaldehyde-fixed cells revealed that CD8-fs380CT showed an intracellular localization

with a significant overlap with PDI and some overlap with ERGIC-53. Most cells also showed some overlap between the CD8-fs380CT and LAMP-1 immunoreactivities (not shown) suggesting that a proportion of the chimera was targeted for degradation in the lysosome before or after reaching the plasma membrane (22).

To test whether the diphenylalanine in fs380CT was also responsible for the localization of CD8-fs380CT, we stably transfected HeLa cells with a chimera in which FF was mutated to AA. In contrast to CD8-fs380CT, CD8-fs380AA immunoreactivity localized to the plasma membrane (Fig. 8*A*).

Surface expression of the CD8 chimeras was assessed by flow cytometry. The fluorescence intensity in cells transfected with the CD8-fs380AA chimera showed a 10-fold increase over that of cells transfected with CD8-fs380CT (Fig. 8*B*), indicating that CD8-fs380AA was about 10 times more efficient in reaching the plasma membrane than CD8-fs380CT.

DISCUSSION

The data presented have shown that the cataract-associated mutant, CX46fs380, did not traffic properly and was retained within the Golgi compartment. Several lines of evidence indicate that the aberrant amino acid sequence of the C terminus of CX46fs380 is responsible for the effects observed: CX46fs380 did not traffic properly whereas a truncated form containing the first 379 amino acids of CX46 (also present in CX46fs380) formed gap junctional plaques; connexin chimeras containing the aberrant sequence of CX46fs380 showed a predominant intracellular distribution; the last 29 amino acids of CX46fs380 were sufficient to cause impaired trafficking of chimeric molecules; and, surface expression of a CD8-fs380CT chimera was markedly decreased.

Acquisition of correct protein conformation is a key step for targeting proteins to the right cellular compartment. The conformation of nascent proteins, and their subsequent processing and transport can be sensitive to temperature. Several disease-associated mutant proteins exhibit temperature-sensitive trafficking (*i.e.* they reach the plasma membrane when incubated at reduced temperatures) (19). Trafficking of CX46fs380 to the plasma membrane was not temperature-sensitive, because gap junctional plaques were not detected after incubation of transfected cells at lower temperatures. Chemical chaperones can also rescue trafficking of some mutant membrane proteins (20). However, 4-phenylbutyrate did not redistribute CX46fs380 to appositional membranes. These results suggest that the trafficking defect in CX46fs380 is not because of a problem in the conformation of the protein.

The export of proteins through the secretory pathway proceeds through a series of directed translocations with formation of cargo-containing vesicles and their fusion from one compartment into the next. These events are directed by signaling elements present in the amino acid sequence of the cargo protein. The observation of the truncated form of CX46, CX46tr380, at gap junctional plaques suggests that the first 379 amino acids of wild-type CX46 are sufficient (while amino acids 380–435 are not essential) for targeting of the protein to gap junctional plaques. Similarly, the first 445 amino acids of CX56 are sufficient for localization at gap junctional plaques.

In many systems the presence of gap junctional plaques correlates with gap junctional conductance. Consistently, in the present study, all connexin constructs that localized at gap junctional plaques formed functional channels. CX46fs380 and chimeras containing fs380CT did not localize at gap junctional plaques and induced significantly reduced junctional currents. The observation that the junctional conductance induced by CX56-fs380CT was significantly higher than that in AS-injected control pairs suggests that the small amount of CX56-fs380CT that reached the plasma membrane was still functional. These results suggest that the reduced

gap junction function of CX46fs380 and connexin chimeras containing fs380CT was caused by improper trafficking of the protein rather than an inability to form functional channels.

Several trafficking motifs (*e.g.* KK*XX*, FF, R*X*R, F(X)$_6$I/LI/L) have been identified within the amino acid sequence of membrane receptors, ER-based proteins and transporters (23–26). ER-based proteins contain a luminal K/HDEL or a dilysine motif in their cytoplasmic C termini (23,27). ERGIC-53, a protein that cycles between the ER and Golgi compartments contains both dilysine and diphenylalanine motifs (28). The last 29 amino acids of fs380CT, which were required for impaired trafficking and function, contain a diphenylalanine and a dilysine-like motif. Our mutational analysis of putative trafficking signals indicated that replacement of the dilysine-like motif with alanines had no effects on protein localization or channel function.

In the present study, two phenylalanines were demonstrated to be critical for the anomalies observed in proteins containing the fs380CT. Their replacement with alanines restored gap junctional plaque localization (and function) to CX46fs380 and the connexin chimeras; it also increased surface expression of the CD8 chimera by about 10-fold. These results suggest that the diphenylalanine in fs380CT acts as a retention signal. This conclusion seems rather paradoxical, because a diphenylalanine motif was initially described as an anterograde transport signal in the p24 family of proteins; the transit of a CD8 chimera from the ER to the Golgi was decreased after replacement of the diphenylalanine with dialanine (24). All members of this family contain a diphenylalanine motif within the cytoplasmic C terminus and localize to the early secretory pathway at steady state (29,30). Similar to the p24 family of proteins, all protein molecules containing fs380CT analyzed in the present study localized to the early secretory pathway at steady state and spent part of their lifetime in the Golgi. However, the exact role of the diphenylalanine as a trafficking signal is unclear. Conflicting effects have been observed after replacement of diphenylalanine with dialanine in several members of this family: impaired anterograde trafficking of chop24 (24), impaired retrieval of p23 from Golgi (31), and increased forward transport of Emp24p from the ER in yeast (32). Moreover, generation of a diphenylalanine by substitution of FF for LL in the ER export motif of the α_{2B}-adrenergic receptor (F(X)$_6$LL) results in a significant decrease in ER to plasma membrane transport (26). Thus, the published data together with our results suggest that an FF signal targets the protein to the early secretory pathway or it acts as a retrieval/retention signal.

The conflicting inferences regarding the role of FF in members of the p24 family of proteins could result from the presence of other trafficking motifs in the protein sequence. A combination of motifs and their amino acid context determine the cellular fate of proteins (24,28,31–35). In chop24, the effect of the FF on transport depends on the presence of a glutamine and a glutamic acid in the transmembrane domain (33). Similarly, Duvernay *et al.* (26) have found that substitution of the F(X)$_6$LL motif with A(X)$_6$FF was necessary to abolish completely ER to plasma membrane trafficking of the α_{2B}-adrenergic receptor. Thus, the FF in CX46fs380 could be part of a more complex motif. However, this possibility seems unlikely, because this sequence originated from a frameshift, not by natural selection. Furthermore, both the immunofluorescence and functional data suggest that the FF is necessary and sufficient to cause impaired protein trafficking. Whereas trafficking signals that direct localization to gap junctional plaques may be present in the truncated form of wild-type CX46 and CX56, they must not be strong enough to overcome the effects of the diphenylalanine present in fs380CT.

In summary, the abnormal C terminus generated as a consequence of the frameshift in CX46 leads to mislocalization of the protein within the secretory pathway and loss of function. The critical residues for these effects are two adjacent phenylalanines. The results suggest that not only loss of targeting signals but also their creation in mutant proteins may lead to disease. This represents a novel mechanism by which mutant proteins can cause disease.

Acknowledgments

We would like to acknowledge Emily Christensen and Meghan McFarlane for their participation in the beginning of these studies.

References

1. Sáez JC, Berthoud VM, Branes MC, Martínez AD, Beyer EC. Physiol Rev 2003;83:1359–1400. [PubMed: 14506308]
2. Hübner CA, Jentsch TJ. Hum Mol Genet 2002;11:2435–2445. [PubMed: 12351579]
3. Reddy MA, Francis PJ, Berry V, Bhattacharya SS, Moore AT. Survey Ophthalmol 2004;49:300–315.
4. Mackay D, Ionides A, Kibar Z, Rouleau G, Berry V, Moore A, Shiels A, Bhattacharya S. Am J Hum Genet 1999;64:1357–1364. [PubMed: 10205266]
5. Pal JD, Liu X, Mackay D, Shiels A, Berthoud VM, Beyer EC, Ebihara L. Am J Physiol Cell Physiol 2000;279:C596–C602. [PubMed: 10942709]
6. Deschenes SM, Walcott JL, Wexler TL, Scherer SS, Fishbeck KH. J Neurosci 1997;17:9077–9084. [PubMed: 9364054]
7. VanSlyke JK, Deschenes SM, Musil LS. Mol Biol Cell 2000;11:1933–1946. [PubMed: 10848620]
8. Matsuyama W, Nakagawa M, Moritoyo T, Takashima H, Umehara F, Hirata K, Suehara M, Osame M. J Hum Genet 2001;46:307–313. [PubMed: 11393532]
9. Di WL, Monypenny J, Common JE, Kennedy CT, Holland KA, Leigh IM, Rugg EL, Zicha D, Kelsell DP. Hum Mol Genet 2002;11:2005–2014. [PubMed: 12165562]
10. Gottfried I, Landau M, Glaser F, Di WL, Ophir J, Mevorah B, Ben-Tal N, Kelsell DP, Avraham KB. Hum Mol Genet 2002;11:1311–1316. [PubMed: 12019212]
11. Thönnissen E, Rabionet R, Arbonès ML, Estivill X, Willecke K, Ott T. Hum Genet 2002;111:190–197. [PubMed: 12189493]
12. Berthoud VM, Minogue PJ, Guo J, Williamson EK, Xu X, Ebihara L, Beyer EC. Eur J Cell Biol 2003;82:209–221. [PubMed: 12800976]
13. Marziano NK, Casalotti SO, Portelli AE, Becker DL, Forge A. Hum Mol Genet 2003;12:805–812. [PubMed: 12668604]
14. Di WL, Gu Y, Common JEA, Aasen T, O'Toole EA, Kelsell DP, Zicha D. J Cell Sci 2005;118:1505–1514. [PubMed: 15769851]
15. Berthoud VM, Beyer EC, Kurata WE, Lau AF, Lampe PD. Eur J Biochem 1997;244:89–97. [PubMed: 9063450]
16. Ebihara L, Beyer EC, Swenson KI, Paul DL, Goodenough DA. Science 1989;243:1194–1195. [PubMed: 2466337]
17. Spray DC, Harris AL, Bennett MVL. J Gen Physiol 1981;77:77–93. [PubMed: 6259274]
18. Ebihara L. Biophys J 1996;71:742–748. [PubMed: 8842212]
19. Denning GM, Anderson MP, Amara JF, Marshall J, Smith AE, Welsh MJ. Nature 1992;358:761–764. [PubMed: 1380673]
20. Rubenstein RC, Egan ME, Zeitlin PL. J Clin Investig 1997;100:2457–2465. [PubMed: 9366560]
21. Nilsson T, Jackson M, Peterson PA. Cell 1989;58:707–718. [PubMed: 2527615]
22. Bonifacino JS, Traub LM. Annu Rev Biochem 2003;72:395–447. [PubMed: 12651740]
23. Jackson MR, Nilsson T, Peterson PA. EMBO J 1990;9:3153–3162. [PubMed: 2120038]
24. Fiedler K, Veit M, Stamnes MA, Rothman JE. Science 1996;273:1396–1399. [PubMed: 8703076]
25. Zerangue N, Schwappach B, Jan YN, Jan LY. Neuron 1999;22:537–548. [PubMed: 10197533]
26. Duvernay MT, Zhou F, Wu G. J Biol Chem 2004;279:30741–30750. [PubMed: 15123661]
27. Munro S, Pelham HR. Cell 1987;48:899–907. [PubMed: 3545499]
28. Kappeler F, Klopfenstein DRCh, Foguet M, Paccaud JP, Hauri HP. J Cell Biol 1997;272:31801–31808.
29. Emery G, Rojo M, Gruenberg J. J Cell Sci 2000;113:2507–2516. [PubMed: 10852829]
30. Jenne N, Frey K, Brügger B, Wieland FT. J Biol Chem 2002;277:46504–46511. [PubMed: 12237308]

31. Nickel W, Sohn K, Bünning C, Wieland FT. Proc Natl Acad Sci U S A 1997;94:11393–11398. [PubMed: 9326620]

32. Nakamura N, Yamasaki S, Sato K, Nakano A, Sakaguchi M, Mihara K. Mol Biol Cell 1998;9:3493–3503. [PubMed: 9843583]

33. Fiedler K, Rothman JE. J Biol Chem 1997;272:24739–24742. [PubMed: 9312065]

34. Dominguez M, Dejgaard K, Füllekrug J, Dahan S, Fazel A, Paccaud JP, Thomas DY, Bergeron JJM, Nilsson T. J Cell Biol 1998;140:751–765. [PubMed: 9472029]

35. Kalandadze A, Wu Y, Fournier K, Robinson MB. J Neurosci 2004;24:5183–5192. [PubMed: 15175388]

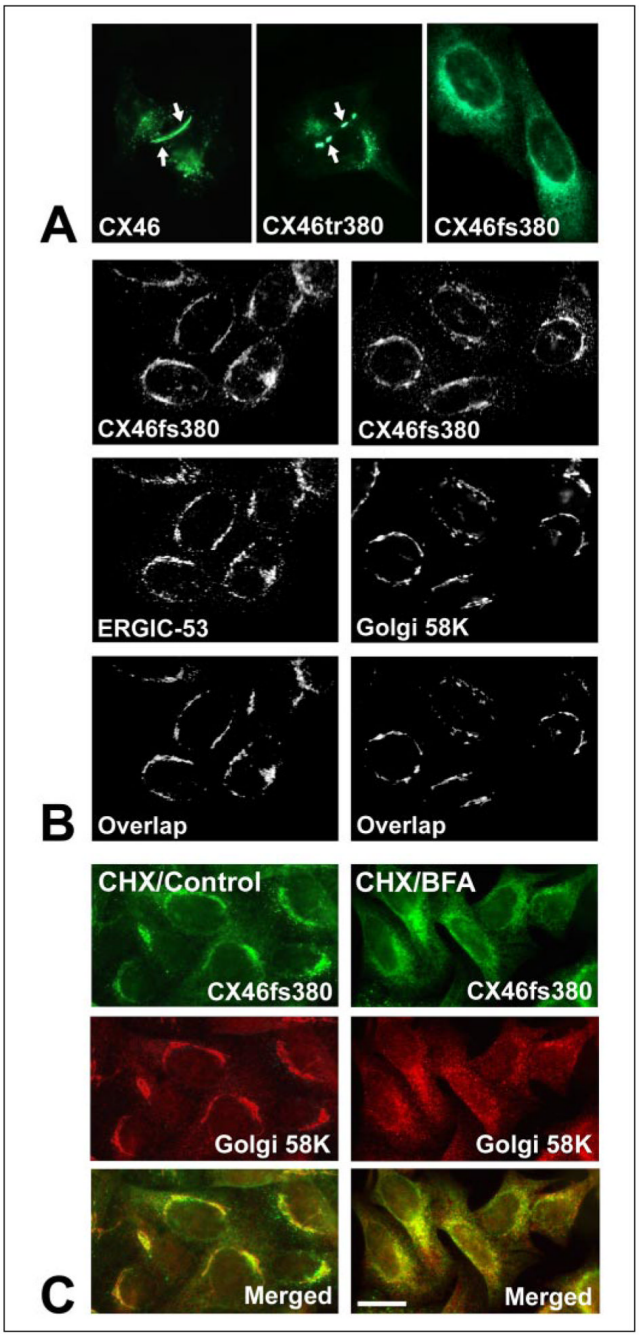

FIGURE 1. Immunoreactive CX46fs380 localizes in the ERGIC and Golgi compartments

A, immunofluorescence of HeLa cells transiently transfected with wild-type CX46 (*CX46*), CX46 truncated after amino acid 379 (*CX46tr380*) or mutant CX46 (*CX46fs380*) after incubation with rabbit anti-CX46IL antibodies and Cy2-conjugated goat anti-rabbit IgG antibodies. Gap junctional plaques are indicated by *arrows. B*, confocal images of HeLa cells stably transfected with CX46fs380 under control conditions after double label immunofluorescence using anti-CX46fs380 antibodies (*top panels*) and a mouse monoclonal anti-ERGIC-53 (*middle left panel*) or anti-Golgi 58K protein (*middle right panel*) antibody; the overlap of the two signals is shown in the *bottom panels. C*, double label immunofluorescence of HeLa cells stably transfected with CX46fs380. Cells were incubated

in the presence of cycloheximide for 16 h by which time negligible amounts of anti-CX46 immunoreactivity could be observed. Then, cells were incubated in the absence (*CHX/Control*) or presence of BFA (*CHX/BFA*). Immunoreactivity to anti-CX46fs380 is shown in *green* and that to anti-Golgi 58K protein is shown in *red*. The merged images are shown at the *bottom*; overlap of the signals appears *yellow*. *Bar*, 20 μm in *A* and *C*; 18 μm in *B*.

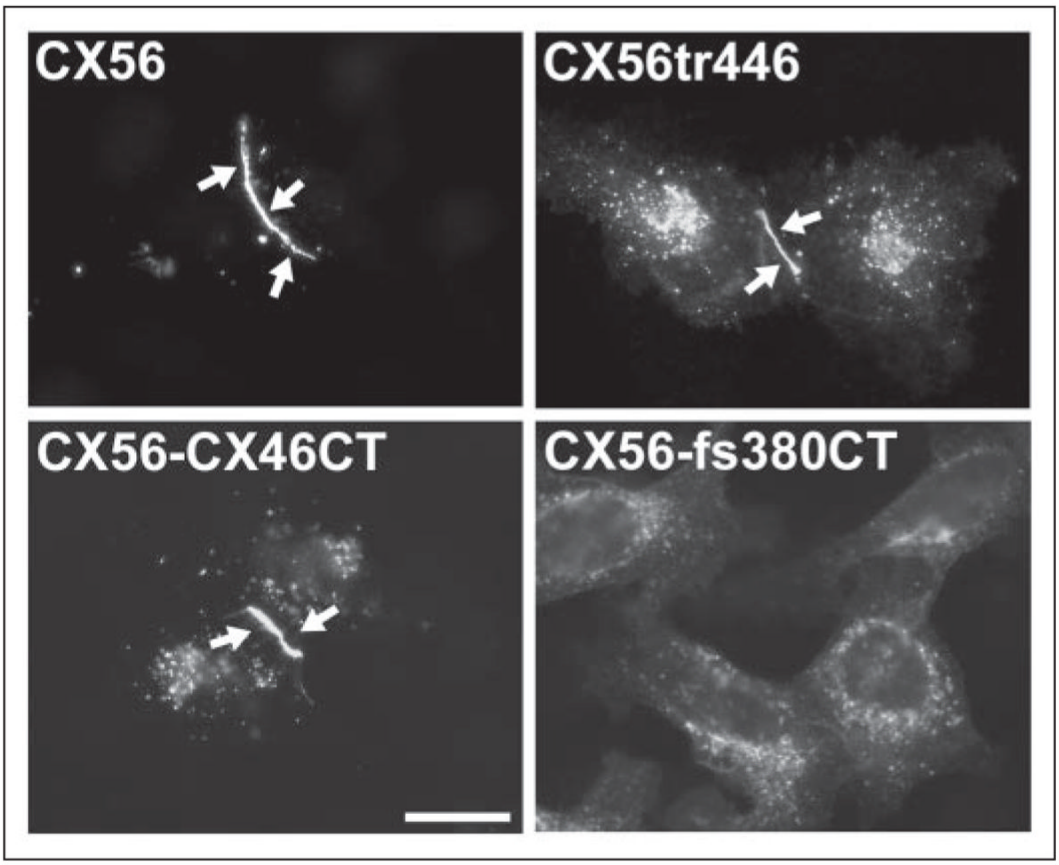

FIGURE 2. Connexin chimeras containing fs380CT exhibit impaired ability to form gap junctional plaques

HeLa cells transiently transfected with CX56 (*CX56*), CX56 truncated after amino acid 445 (*CX56tr446*) or CX56 chimeras containing the first 445 amino acids of CX56 and amino acids 380 – 435 of the C terminus of CX46 (*CX56-CX46CT*) or the aberrant sequence of CX46fs380 (*CX56-fs380CT*) were subjected to immunofluorescence using anti-CX56CT antibodies and Cy2-conjugated goat anti-rabbit IgG antibodies. Gap junctional plaques are indicated by *arrows. Bar*, 20 μm.

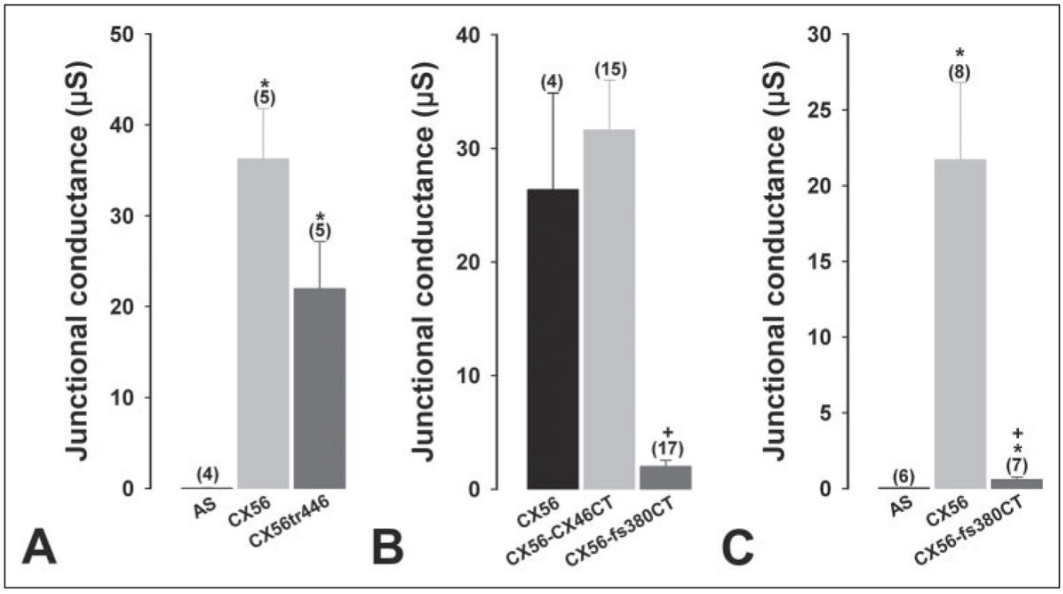

FIGURE 3. The CX56-fs380CT chimera is impaired in its ability to form functional gap junction channels

A–C, junctional conductances in pairs of *Xenopus* oocytes injected with cRNAs coding for CX56, CX56tr446, CX56-CX46CT, or CX56-fs380CT were determined by double whole cell voltage clamp. All oocytes were injected with antisense oligonucleotides (*AS*) to block endogenous Cx38 junctional currents. Data are presented as the mean ± S.E. The number of pairs is indicated in *parentheses*. *, $p < 0.001$ compared with AS-injected oocyte pairs; +, $p < 0.001$ when comparing CX56- or CX56-CX46CT-injected oocyte pairs with CX56-fs380CT-injected oocyte pairs.

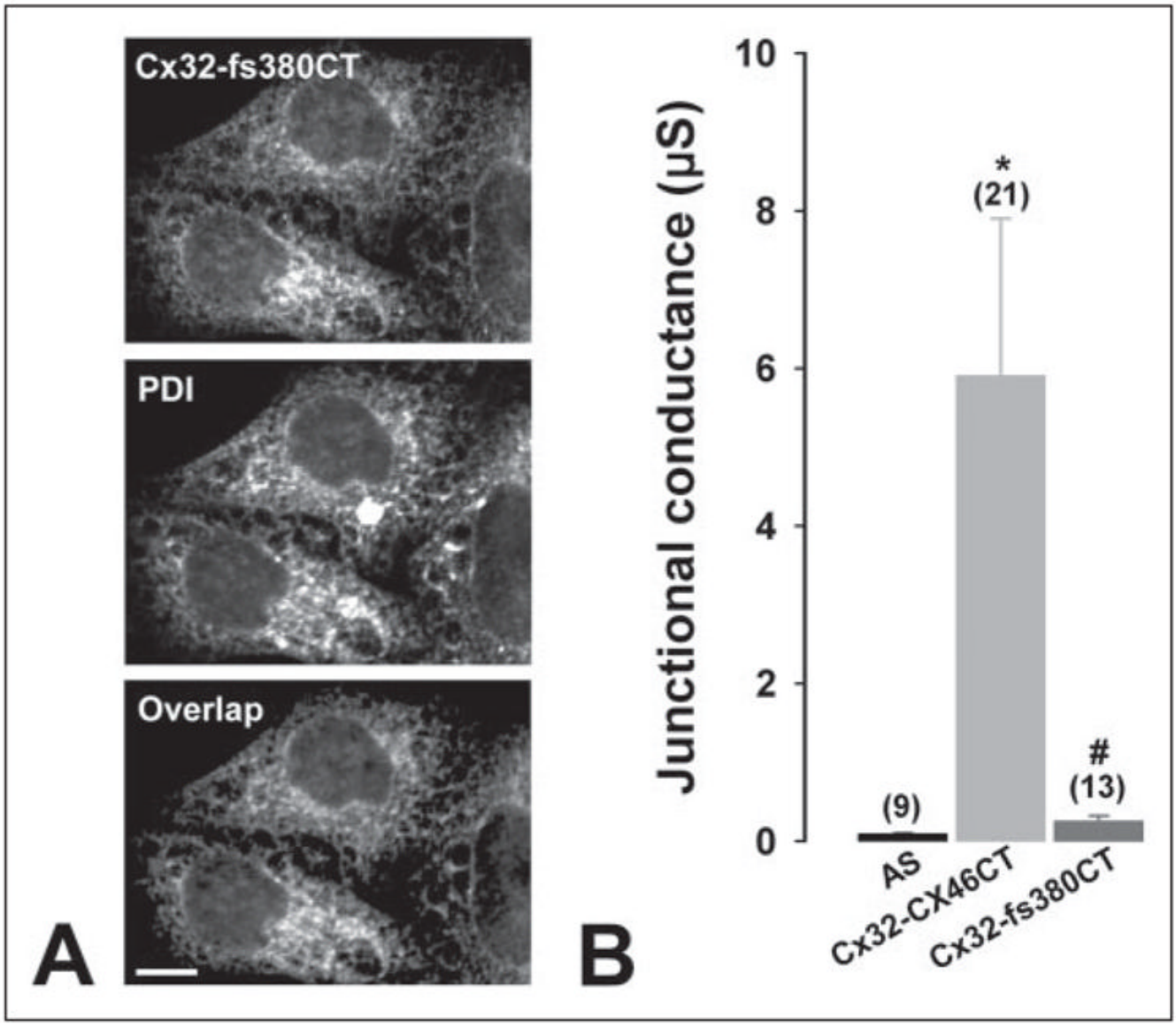

FIGURE 4. A Cx32 chimera containing fs380CT is impaired in its capacity to form gap junctional plaques and induce junctional conductance

A, confocal images of HeLa cells stably transfected with Cx32-fs380CT after double label immunofluorescence using rabbit polyclonal anti-CX46fs380 antibodies (*top panel*) and a mouse monoclonal anti-PDI antibody (*middle panel*); the overlap of the two signals is shown on the *bottom panel*. *B*, junctional conductances in pairs of *Xenopus* oocytes injected with cRNAs coding for Cx32-CX46CT or Cx32-fs380CT were determined by double whole cell voltage clamp. Data are presented as the mean ± S.E. The number of pairs is indicated in *parentheses*. *, $p < 0.001$ compared with AS-injected oocyte pairs; #, $p < 0.001$ when comparing Cx32-CX46CT-injected oocyte pairs with Cx32-fs380CT-injected oocyte pairs. *Bar*, 10 μm.

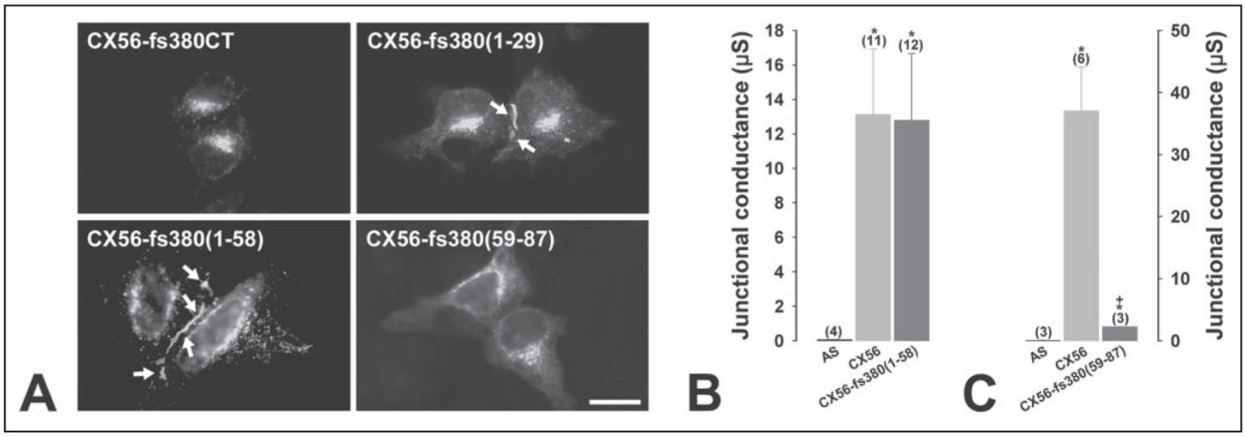

FIGURE 5. The last 29 amino acids of the aberrant sequence of CX46fs380 are sufficient to induce loss of immunoreactivity at appositional membranes and loss of function

A, immunofluorescence of HeLa cells transiently transfected with CX56-fs380CT or chimeras containing the first one-third of fs380CT *(CX56-fs380(*1–29)), the first two-thirds of the fs380CT sequence *(CX56-fs380(1–58))* or the last one-third *(CX56-fs380(59 – 87))* using rabbit anti-CX56CT antibodies and Cy2-conjugated goat anti-rabbit IgG antibodies. Gap junctional plaques are indicated by arrows. *B* and *C*, graphs showing the junctional conductances determined by double whole cell voltage clamp in pairs of *Xenopus* oocytes injected with CX56, CX56-fs380(1–58) or CX56-fs380(59 – 87) cRNAs. The data are presented as the mean ± S.E. The number of pairs is indicated in *parentheses*. *, $p < 0.001$ compared with AS-injected oocyte pairs; +, $p < 0.001$ when comparing CX56-injected oocyte pairs with CX56-fs380(59 – 87)-injected oocyte pairs. *Bar*, 20 μm.

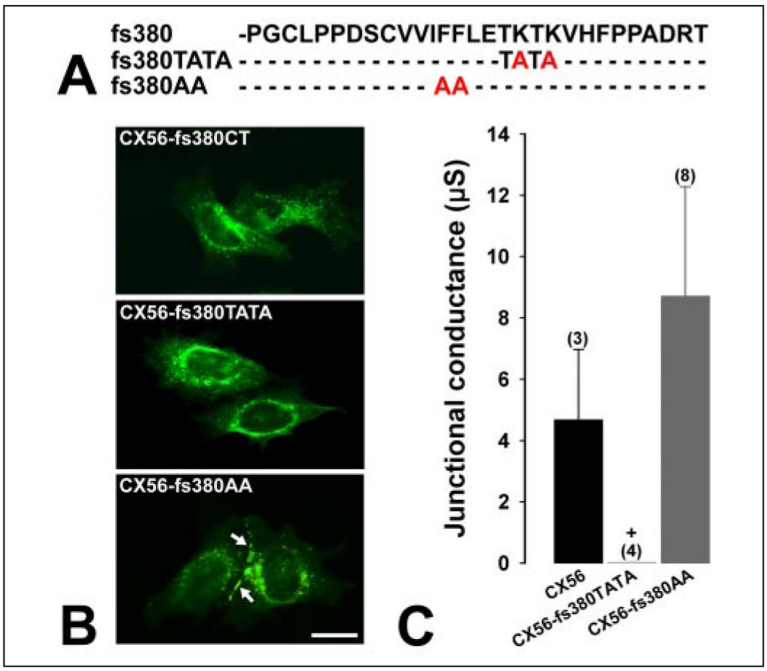

FIGURE 6. A diphenylalanine in fs380CT is responsible for the aberrant localization and loss of function of CX56 chimeras

A, sequence of the last 29 amino acids of CX46fs380 (*top line*) and positions of the amino acids that were mutated to alanines (in *red*) to generate the fs380TATA and fs380AA mutant chimeras. *B*, immunofluorescence of HeLa cells transiently transfected with CX56-fs380CT or chimeras containing the aberrant sequence of CX46fs380 with two lysines (*CX56-fs380TATA*) or phenylalanines (*CX56-fs380AA*) substituted with alanines using rabbit anti-CX56CT antibodies and Cy2-conjugated goat anti-rabbit antibodies. Gap junctional plaques are indicated by *arrows*. *C*, *graph* showing the junctional conductances in pairs of *Xenopus* oocytes injected with CX56, CX56-fs380TATA, or CX56-fs380AA cRNAs. The data are presented as the mean ± S.E. of the number of pairs indicated in *parentheses*. +, $p < 0.005$ when comparing CX56-with CX56-fs380TATA-injected oocyte pairs. *Bar*, 20 μm.

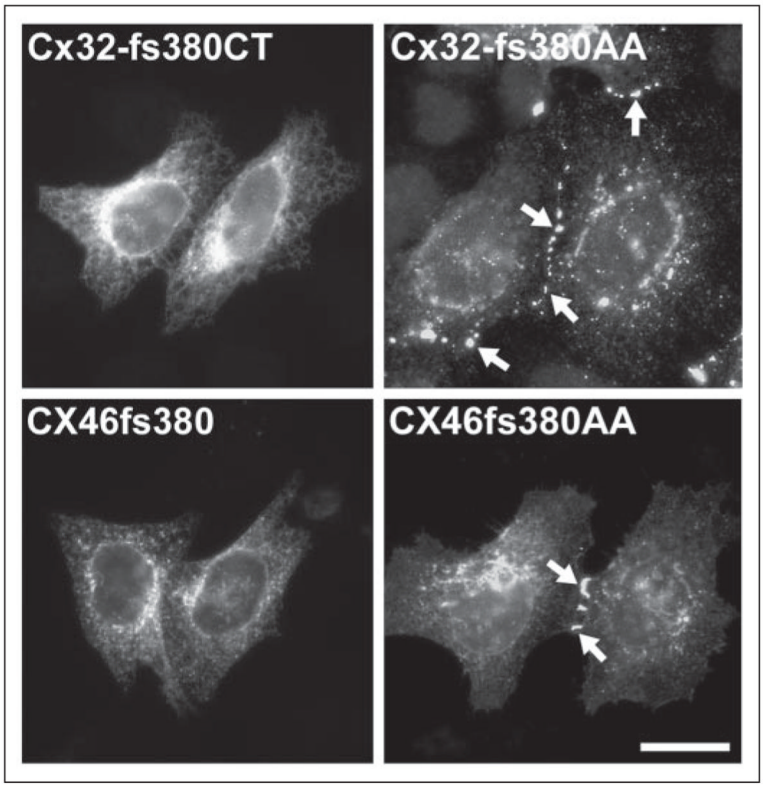

FIGURE 7. Substitution of FF for AA restores membrane localization and function to a Cx32 chimera and CX46fs380

Immunofluorescence of HeLa cells transiently transfected with Cx32-fs380CT, Cx32-fs380AA (a chimera in which the diphenylalanines in fs380CT were mutated to dialanine), CX46fs380 or CX46fs380AA. Binding of rabbit polyclonal anti-Cx32 or anti-CX46IL antibodies was detected with Cy2-conjugated goat anti-rabbit IgG antibodies. Gap junctional plaques are indicated by *arrows. Bar*, 20 μm.

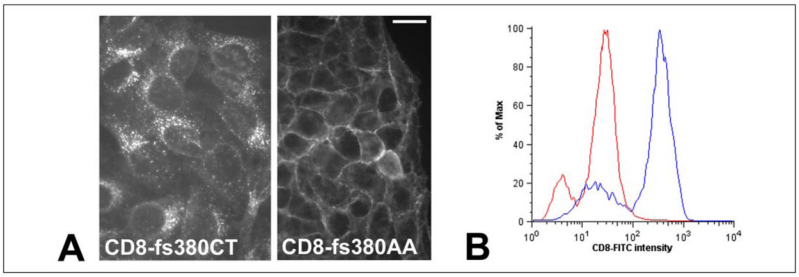

FIGURE 8. The diphenylalanine in fs380CT causes retention of a CD8 chimera

A, immunofluorescence of stably transfected HeLa cells showing the distribution of CD8 chimeras in which the cytoplasmic domain of CD8 was replaced with fs380CT (*CD8-fs380CT*) or with an fs380CT in which two alanines replaced the diphenylalanine (*CD8-fs380AA*). Localization of CD8 chimeras was detected using a FITC-conjugated antibody against the extracellular N terminus of CD8. *B*, graph illustrating the surface expression of CD8-fs380CT (*red*) and CD8-fs380AA (*blue*) measured by flow cytometry. *Bar*, 20 μm.

TABLE ONE

List of primers

Primer number	Sequence
1	5′-AAGCTTGCCGCCACCATGGGCGACTGGAGCTTTCTGGGA-3′
2	5′-TCTAGATCAGCCGCTCCCATCCAGCAGCAG-3′
3	5′-TGAGAATTCGCCACCATGGGTGACTGGAGCTT-3′
4	5′-TCTAGACTAGCCACTGTTGGTTGTGGTGATG-3′
5	5′-GCTTCCGGAGTTGGTTGTGGTGATGGGCGGCCC-3′
6	5′-GGGTCCGGAAGCAGTCTGGAGGGGAGCGCCCTG-3′
7	5′-GGGTCCGGACAGCAGTCTGGAGGGGAGCGC-3′
8	5′-GATCGAATTCGATTTCATCAGGTTCTATCTGCTGG-3′
9	5′-GCCGCCACCATGAACTGGACAGGTCTATACACC-3′
10	5′-CTGCTGTCCGGAGCAGGCTGAGCATCGGTCGCTCTTCTCAGC-3′
11	5′-TTATCAGGCGGCTGGTGCATCTGGGCCGCGGTG-3′
12	5′-TTATCACACTAGATGGCCAAGTCCTCCGGTCTG 3′
13	5′-ATATCCGGACCCGGGTGCCTGCCTCCAGAC-3′
14	5′-TCAGGTTCTATCTGCTGGTGGGAAGTGCACTTTGG-3′
15	5′-GAGACCGCTACCGCTGTGCACTTCCCACCAGCAGATAGAACC-3′
16	5′-GAGGAAAAAGATCACTACACAGCTGTCTGGAGGCAGGCACCC-3′
17	5′-GAGACCAAAACCAAAGTGCACTTCCCACCAGC-3′
18	5′-GAGAGCAGCGATCACTACACAGCTGTCTGGAGGC-3′
19	5′-GTCATGGCCTTACCAGTGACCGCCTTG-3′
20	5′-CTGCTGTCCGGAGTTGCAGTAAAGGGTGATAAC-3′

TABLE TWO

Preparation of connexin chimeras and substitution mutants

Name of construct	Procedure for construct preparation	DNA fragment	Procedure for DNA fragment preparation	Primer set[a]
CX46tr380	PCR using wild-type CX46 as template			1 and 2
CX56tr446	PCR using wild-type CX56 as template			3 and 4
CX56-CX46CT	Ligation of CX56-445-BspEI to wild-type CX46CT-BspEI	CX56-445-BspEI	PCR using wild-type CX56 as template	3 and 5
		CX46CT-BspEI	PCR using wild-type CX46 as template	6 and 8
CX56-fs380CT	Ligation of CX56-445-BspEI to fs380CT-BspEI	CX56-445-BspEI	PCR using wild-type CX56 as template	3 and 5
		fs380CT-BspEI	PCR using CX46fs380 as template	7 and 8
Cx32-CX46CT	Ligation of Cx32-BspEI to wild-type CX46CT-BspEI (This construct contains amino acids 378–435 of wild-type CX46)	Cx32-BspEI	PCR using wild-type rat Cx32 as template	9 and 10
		CX46CT-BspEI	PCR using wild-type CX46 as template	6 and 8
Cx32-fs380CT	Ligation of Cx32-BspEI to fs380CT-BspEI (This construct contains amino acids 378–466 of CX46fs380)	Cx32-BspEI	PCR using wild-type rat Cx32 as template	9 and 10
		fs380CT-BspEI	PCR using CX46fs380 as template	7 and 8
CX56-fs380(1–29)	PCR using CX56-fs380CT as template			3 and 11
CX56-fs380(1–58)	PCR using CX56-fs380CT as template			3 and 12
CX56-fs380(59–87)	Ligation of CX56-445-BspEI to fs380CT(59–87)	CX56-445-BspEI	PCR using wild-type CX56 as template	3 and 5
		fs380CT(59–87)	PCR using CX46fs380 as template	13 and 14
CX56-fs380TATA	PCR using CX56-fs380CT as template			15 and 16
CX56-fs380AA	PCR using CX56-fs380CT as template			17 and 18
Cx32-fs380AA	PCR using Cx32-fs380CT as template			17 and 18
CX46fs380AA	PCR using CX46fs380 as template			17 and 18
CD8-fs380CT	Ligation of CD8-BspEI to fs380CT-BspEI	CD8-BspEI	PCR using CD8 as template	19 and 20
		fs380CT-BspEI	PCR using CX46fs380 as template	7 and 8
CD8-fs380AA	PCR using CD8-fs380CT as template			17 and 18

[a] Primers 5, 6, and 7 incorporate a BspEI site by silent mutation of codons 444–445 of CX56, 378–379 of CX46 and CX46fs380 to TCC-GGA. Ligation of PCR products obtained using primers 15 and 16 or 17 and 18 generates an XhoI site by building a silent mutation from TTA-GAA to CTC-GAG at codons 452–453 of CX46fs380.